Miranda, E., Garzón, C., Martínez-Cisneros, C.S., Alonso, J., García-García, J. (2012). Detection and characterization of the spatial inhibition potential in electroperforated sheet materials, *Journal of Electrostatics*, 70(3), pp.: 264-268.

DOI: https://doi.org/10.1016/j.elstat.2012.03.004

Detection and characterization of the spatial inhibition potential in electroperforated sheet materials

E. Miranda , C. Garzón, C.S. Martínez-Cisneros, J. Alonso, J. García-García

The spatial distribution of tiny holes in sheet materials generated by means of electrical discharges is investigated using spatial statistics techniques. It is shown that whereas the holes appear to be randomly distributed according to a Poisson point pattern, there is in fact a small region around each hole in which the generation of a new one is statistically inhibited as a consequence of the lower impedance path offered by the already made hole. The resulting pattern is known in spatial statistics as a point process with a soft core inhibition potential, which can be characterized using the pair correlation function.

1. Introduction

Electroperforation is a widespread method used in industry to generate a high density of tiny holes in separate sheets or web materials [1]. The sheet material often moves at a high speed through the spark gap of a single or multiple pairs of needle like opposed electrodes while the holes are created by means of a continuous train of electrical discharges. The method is applied for obtaining ventilated paper bags and cigarette tipping paper with the required air permeability properties. The main interest in perforating a sheet material is to facilitate the air flow through it and, because of esthetic reasons, it is sometimes desirable that the holes are invisible to the naked eye. This latest requirement poses a serious constraint on the perforation process since the discharge power must be always kept under controlled conditions. However, a major limitation of this perforation technique is that there is a maximum number of holes that can be generated per unit area due to the fact that the already made holes offer easier discharge paths between the electrodes. This self limiting hole generation process does not allow increasing the material porosity beyond a certain level even under longer exposure times (lower velocities of the sheet material) or higher discharge frequencies (limited by the recovery time of the electronic system). In a previous paper [2], we showed this effect to occur in 1D perforation tracks and the minimum distance between consecutive holes was called the drag distance. This parameter also plays a key role in determining the maximum density of holes than can be achieved in sheet materials.

In this work, the 2D spatial distribution of perforations in paper sheets is investigated using spatial statistics techniques [3]. The characterization method described here can be easily extended to a number of thin materials susceptible of being electrically perfo rated like leather, leatherine, packaging foils, coatings and even biological membranes for drugs delivery [1]. It is assumed for the analysis that the properties of the sheet material do not change from location to location so that the hole distribution can be mathematically regarded as a truly 2D point process. In our case, we will neglect the roled played by the fiber distribution in paper sheets, which is considered to be totally random. However, it should be kept in mind that, since the holes are generated sequentially, the particular features of the hole generation method can also have some influence on the final distribution. The analysis of such a time dependent process is complex and requires space time models [3] that are out of the scope of this paper.

Briefly, the aims of point process statistics are to describe the locations of randomly distributed objects in 1, 2, or 3D space and, if possible, to understand the mutual interactions that led to that distribution [4]. Quite often there is a special interest in detecting clustering (aggregation) or repulsion effects between the points, as

well as the distance scales involved, with the purpose of inferring the underlying mechanism responsible for the formation of the pattern. This kind of analysis involves a number of statistical tools such as intensity plots, empirical and theoretical distance histo grams and functional summary estimators like the Ripley's K function and its derivative, the pair correlation function. It is worth mentioning that the standard reference model of a point process is the homogeneous Poisson point process with intensity λ, where λ, in our case, is the expected number of points per unit area. This process is referred to as the Complete Spatial Randomness (CSR) process and is commonly regarded as the null hypothesis model in spatial statistics [3]. As it will be shown below, although the hole distribution in paper sheets seems to follow a CSR process when analyzed in a sufficiently large area, the hole pattern considerably departs from that behavior for short distances, where a lower number of events than that expected for a CSR process is counted. This sort of short range repulsion effect between holes can be quantified in terms of the so called inhibition potential. In a previous work [5], we also call the attention on this interpoint interaction and therein the hole distribution was assessed using the quadrat counts method in combination with the Morishita index. On that occasion, it was demonstrated that conclusions drawn from interpoint analysis can be largely affected by the choice of the quadrat size, which is an undesirable feature from the statistical viewpoint. Here, instead, distance methods, which rely on the relative position of the points within an observation window, are applied to investigate the hole distribution thoroughly.

2. Experimental set up and statistical tools

In order to investigate the 2D distribution of holes in sheet materials, a simple two electrode discharge set up was imple mented (see Fig. 1.a). The sparks were generated using an IGBT (Isolated Gate Bipolar Transistors) based circuit consisting of a two stage multiplier (500V $\times$ 2 stages) whose output is a train of pulses with controlled amplitude and frequency. The output at the spark gap between the electrodes is a high voltage train of pulses with a wide frequency range (typically from a few Hz to 15 kHz). The electrodes are tungsten needles and the perforated material is 80 g/m^2 paper sheet. The separation between the tips of the electrodes is 3 mm and it is set using precision micropositioners. Two inde pendent programmable step motors control the movement of the perforation window. In order to ensure a complete coverage of the area of interest, the perforation window is displaced horizontally and vertically as illustrated in Fig. 1.b. Notice that although the motors cause the discrete motion of the sheet material, the stochastic nature of the discharge paths introduces randomness in the hole generation process. Further details about the experimental set up can be found in Ref. [6].

Once the hole pattern is generated, the second step consists in characterizing the hole distribution by means of exploratory statistical techniques. To this aim, the Spatstat package for R language has been utilized [7]. R is a free software environment for statistical computing and Spatstat is one of its contributed pack ages. Spatstat has been developed mainly by Prof. A. Baddeley and Prof. R. Turner and is a specific package designed to be used for spatial data manipulation, exploratory data analysis, simulation, fitting and model diagnostics. All the statistical plots shown in this work were generated using this software.

2.1. Analysis and discussion

As described in the previous Section, a hole pattern in a paper sheet can be generated under controlled conditions. As schemat ically depicted in Fig. 2, the sheet is placed in the spark gap and is

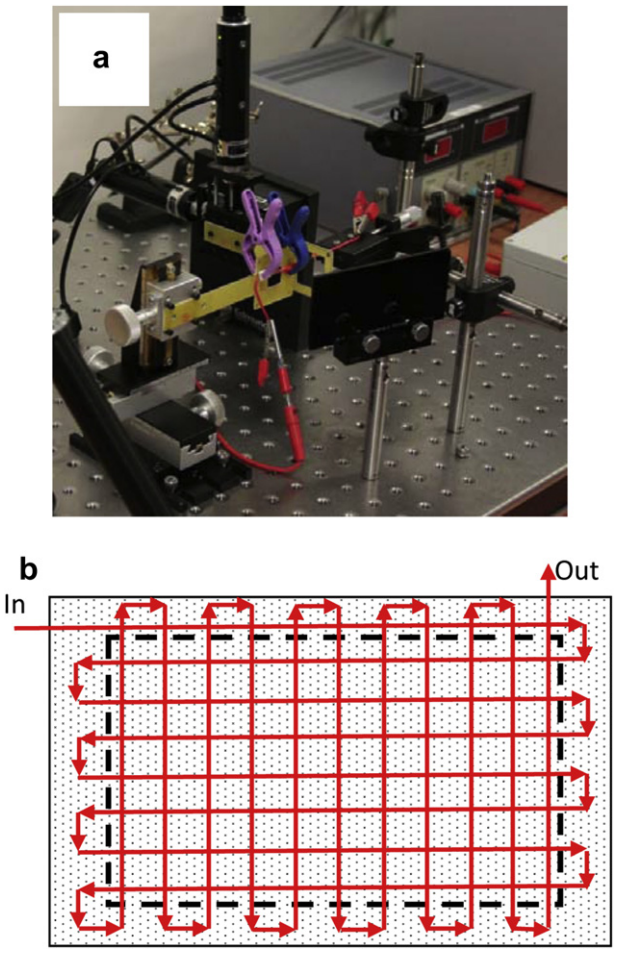

Fig. 1. a) Photograph of the perforation set up. The perforation window is vertically and horizontally shifted using two computer-controlled motors. b) Simplified movement of the perforation window. The red solid line indicates the path followed by the needle-like electrodes. (For interpretation of the references to colour in this figure legend, the reader is referred to the web version of this article.)

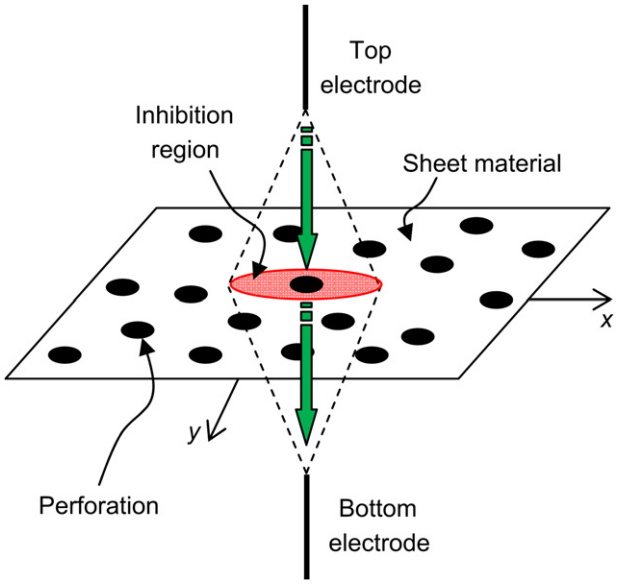

Fig. 2. Simplified scheme of the electroperforation process. The sheet material moves in the x- and y-directions. Each hole (dark circles) defines an inhibition region (shaded area) in which no other hole can be generated. The thick vertical arrows show a direct electrical discharge between the top and bottom electrodes.

synchronously moved in the x and y directions using computer controlled step motors. The shaded area represents the inhibi tion region described below. Fig. 3.a illustrates a typical distribu tion of holes obtained by this procedure. In this particular case, N 1486 points were generated with an average intensity λ 151 points/mm^2. The size of the observation window is a 2.71 mm x b 3.62 mm. Notice that the hole sizes are not identical and this is presumably so because multiple sparks have passed through the same hole during the x–y sweeps. Typical sizes are in the range from 10 to 20 μm. The analysis of marked point processes (hole sizes in this case) is also matter of study of spatial statistics but this problem is out of the scope of the present analysis. Fig. 3.b is the intensity plot associated with Fig. 3.a, *i.e.* the expected number of points per unit area calculated using an isotropic Gaussian kernel of fixed bandwidth (Δ 0.04 mm). The intensity or first moment of a point process is the analog of the expected value of a random variable [7]. For this particular realization the intensity is not homogeneous but this is a characteristic of a CSR process. The histograms in Fig. 4 reveal that the x and y coordinate values of the points shown in Fig. 3.a are uniformly distributed in agreement with a 2D Poisson distribution. Recall that a Poisson point process not only yields uniformly distributed x and y coordinate values but requires a Poisson distributed number of events in any subregion [3].

Since we are interested in detecting any kind of interaction between the points, as a first step, the interevent distances will be analyzed. Fig. 5 shows the distance histograms for all the points laying within the observation window $a \times b$. It is worth mentioning

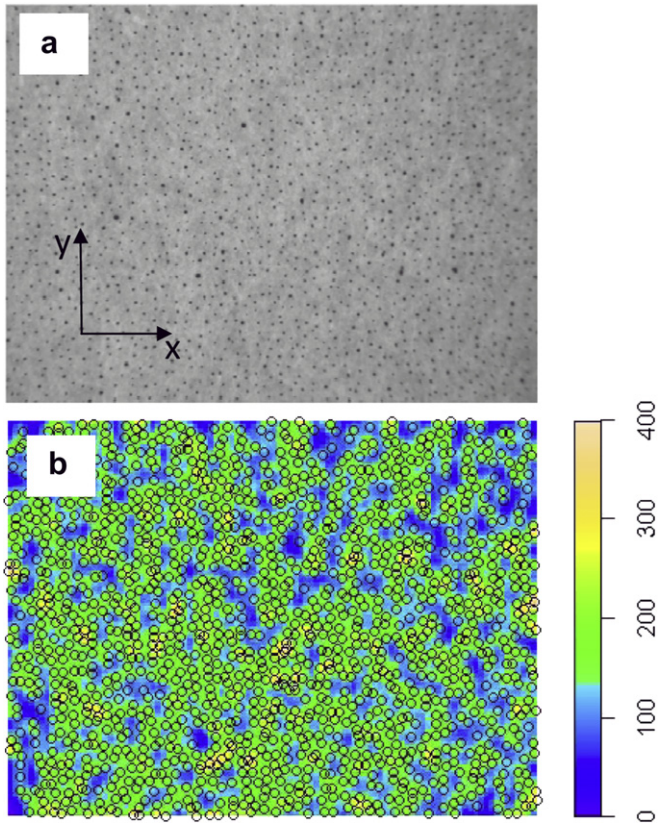

Fig. 3. a) Photograph of an electroperforated paper. The size of this region is a 2.71 mm $\times$ b 3.62 mm ,b) Intensity plot for the perforations shown in a). This plot helps to identify anomalies in the hole generation process. In this particular case, N 1486 points were generated with an average intensity λ 151 points/mm^2. The right scale shows the local intensity of the process.

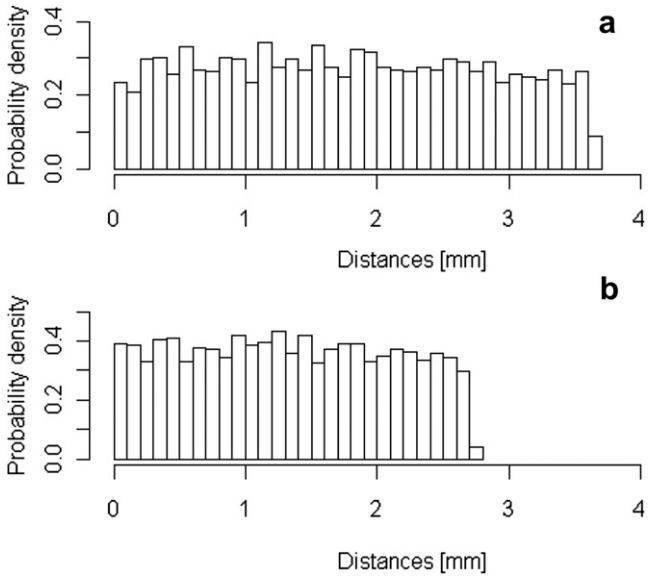

Fig. 4. Empirical histograms for the hole locations shown in Fig. 3.a in the a) x-direction and, b) y-direction. These plots helps to assess the uniformity of the x- and y-coordinate distributions for the hole locations.

that the observed pairwise distances x_{ij} $||\mathbf{x}_i \ \mathbf{x}_j||$ $(i \neq j)$ constitute a biased sample of the point process, with a bias in favor of the smaller distances (pairwise distances greater than the diagonal of the rectangle cannot be observed). Since there are N points, the number of distances represented in this histogram is $N(N \ 1)/2$. For the case under investigation, this is more than one million data. The theoretical expression for the probability distribution of a CSR point process in a rectangle is given by [8]:

$$f_{\mathrm{CSR}}(x) \quad \frac{4x}{a^2 b^2}\Phi(x) \tag{1}$$

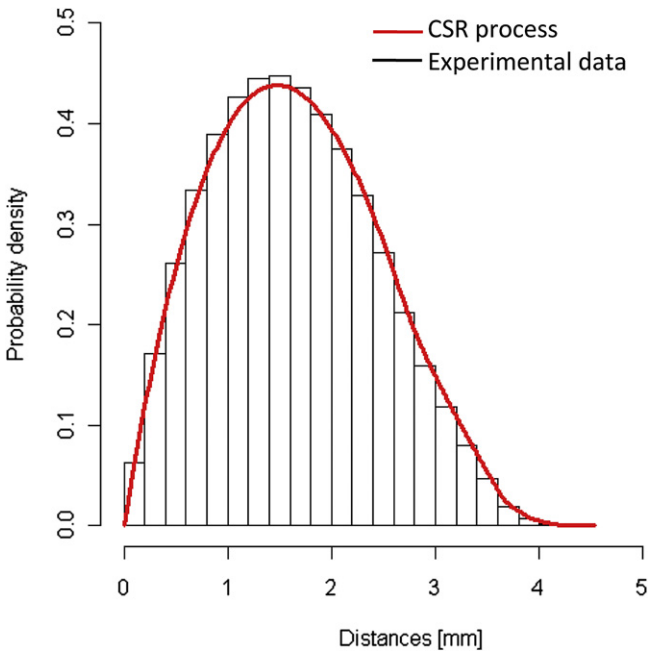

Fig. 5. Histogram and theoretical probability density for the interpoint distances of the holes shown in Fig. 3.a. The solid line was calculated using expressions (1) and (2).

where

$$\Phi(x) \quad \begin{cases} \dfrac{ab\pi}{2} \quad (a+b)x + \dfrac{x^2}{2} & 0 < x < a \\ ab\sin^{-1}\left(\dfrac{a}{x}\right) \quad \dfrac{a^2}{2} + b\sqrt{x^2} \quad a^2 \quad bx & a < x < b \\ ab\left(\sin^{-1}\left(\dfrac{a}{x}\right) \quad \sin^{-1}\left[\sqrt{1 \quad \dfrac{b^2}{x^2}}\right]\right) \quad \dfrac{x^2}{2} + a\sqrt{x^2} \quad b^2 + b\sqrt{x^2} \quad a^2 \quad \dfrac{(a^2+b^2)}{2} & b < x < \sqrt{a^2+b^2} \end{cases} \tag{2}$$

which is represented by the solid line in Fig. 5. A transcription error has been detected in Eq. (3) Ref [8]. (the term $-bx$ is missing) and has been corrected in Eq. (2) of this work. Notice that the agree ment between the theoretical curve and the empirical histogram is excellent what could lead us to think that the holes follow a CSR process for all length scales. However, the histogram corresponding to the nearest neighbor distances $w_i \quad \min_{j\neq i} x_{ij}$ shown in Fig. 6 reveals that this is not the case. The solid line in Fig. 6.a is the theoretical probability distribution corresponding to the nearest neighbor distances for a CSR point process [4]:

$$h_{\mathrm{CSR}}(w) \quad 2\lambda\pi w \exp(\ \lambda\pi w^2) \tag{3}$$

Typical hole sizes and distances are shown in Fig. 6.b. For $\lambda \quad 151$ points/mm^2, the maximum of $h_{\mathrm{CSR}}(w)$ occurs for $w \quad 0.035$ mm, whereas the maximum of the histogram is obtained for $w \quad 0.065$ mm, which nearly doubles the theoretical value. This indicates that the shortest distances between holes expected for a CSR process are not represented in the histogram of Fig. 6. This poses a warning on the actual distribution of the generated holes and motivates the following analysis.

In order to improve our understanding about why a deviation from CSR is observed, a common procedure is to analyze the available data using functional summary statistics rather than direct distance methods as we did above. To this end, the Ripley's K function has been considered first. The K function is defined as [3]:

$$K(r) \quad \lambda^{-1} \cdot E(\text{number of events within a distance r of an arbitrary event}) \tag{4}$$

where E is the expectation operator. This function is also called the reduced second moment measure because it is related to the second order intensity of a stationary isotropic point process [4]. For a CSR process, $K(r)$ simply reads:

$$K_{\mathrm{CSR}}(r) \quad \pi r^2 \tag{5}$$

which is independent of λ. This function is plotted in Fig. 7.a using an isotropic correction estimate [7]. Notice that any deviation from the parabolic behavior predicted by Eq. (5) can hardly be seen in that plot. A commonly used transformation of K is the L function defined as:

$$L(r) \quad \sqrt{\frac{K(r)}{\pi}} \tag{6}$$

so that

$$L_{\mathrm{CSR}}(r) \quad r \tag{7}$$

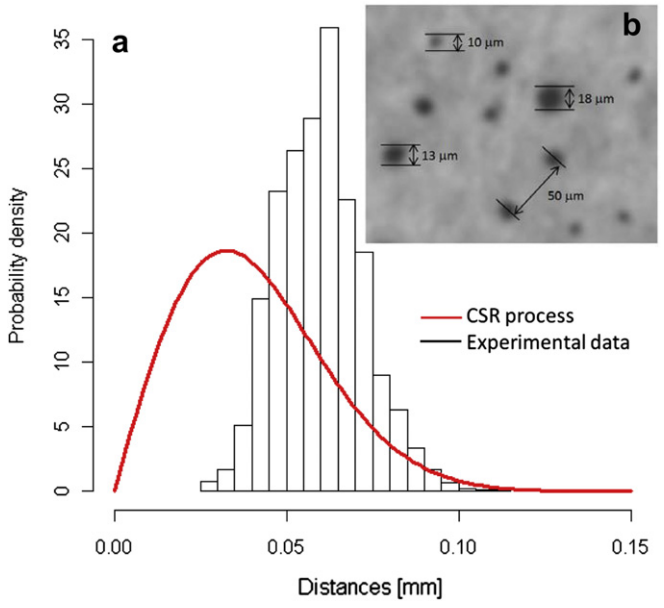

Fig. 6. a) Histogram and theoretical probability density for the nearest neighbor distances of the holes shown in Fig. 3.a. The solid line was calculated using expression (3). b) Detail of a perforated region showing typical hole sizes and distances.

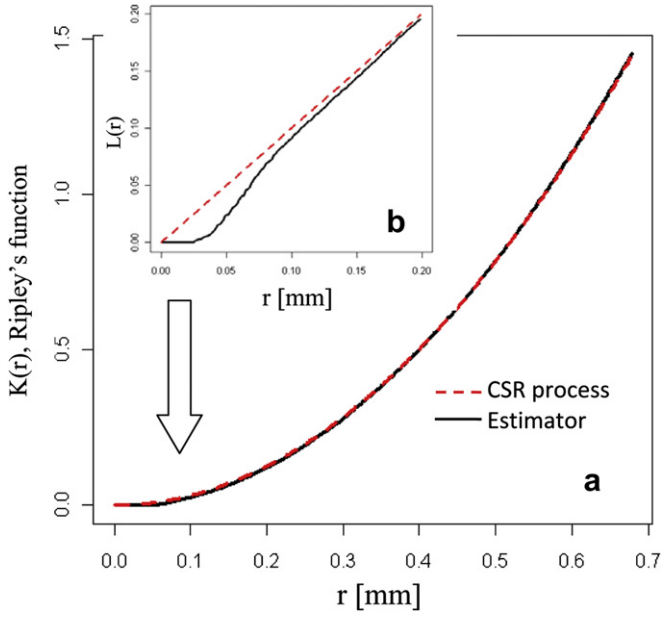

Fig. 7. a) Ripley's K function plot for the empirical data (solid line) and theoretical (dashed line) expression (5). b) Detail of a) For very small distances using the transformation (6). Notice the departure (inhibition) from a CSR process.

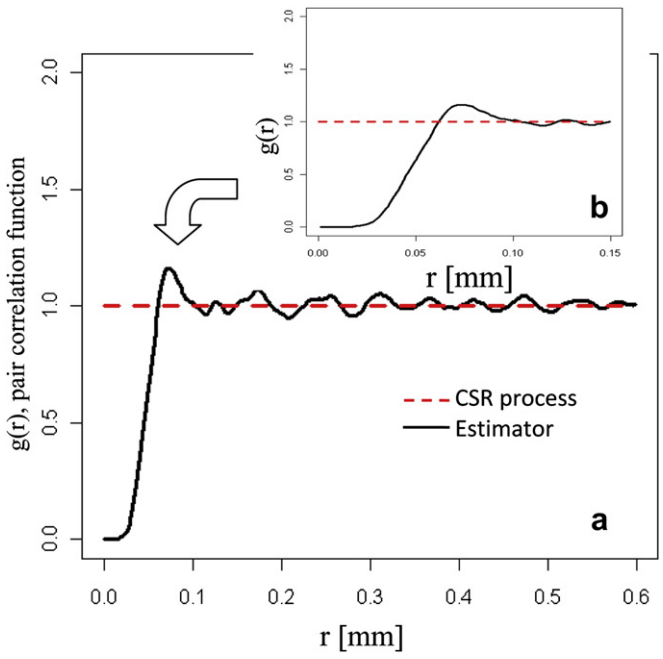

Fig. 8. a) Pair correlation function plot for the empirical data (solid line) and theoretical (dashed line) expression (8). b) Detail of a) For very small distances. Notice the departure (inhibition) from a CSR process.

The square root transformation (6) not only makes visual assessment of the graph easier but also stabilizes the variance of the K estimator [7]. The fact that the empirical estimator shown in Fig. 7.b (solid line) is below the theoretical L curve (dashed line) reveals that the number of holes closer than 0.075 mm is lower than what is expected for a CSR process. Closely related to K function is the pair correlation function g, which is defined as:

$$g(r) \quad \frac{1}{2\pi r}\frac{\mathrm{d}K(r)}{\mathrm{d}r} \tag{8}$$

$g(r)$ is nothing but the probability of observing a pair of points separated by a distance r divided by the corresponding proba bility for a Poisson process. $g(r)$ 1 corresponds to a CSR process, while $g(r) > 1$ suggests clustering or attraction at distance r and $g(r) < 1$ suggests inhibition or regularity. The pair correlation function g is considered for several authors the most informative second order summary characteristic for spatial point processes [3]. As illustrated in Fig. 8, the function g reveals again that there is an inhibition region around each point of typical size 0.075 mm. The fact that the transition from the inhibition region ($g \approx 0$) to the CSR region ($g \approx 1$) takes place gradually indicates that we are dealing with a soft core potential with statistically distributed inhibition distances ranging from r_{in} 0.050 mm to r_{out} 0.075 mm (see Fig. 9.b). The observed effect is typical of a Strauss process with pairwise interaction [7] and is illustrated by the three shaded regions in Fig. 9.a. The existence of this inhibition region sheds light on one of the major limitations of the electroperforation process of thin porous materials.

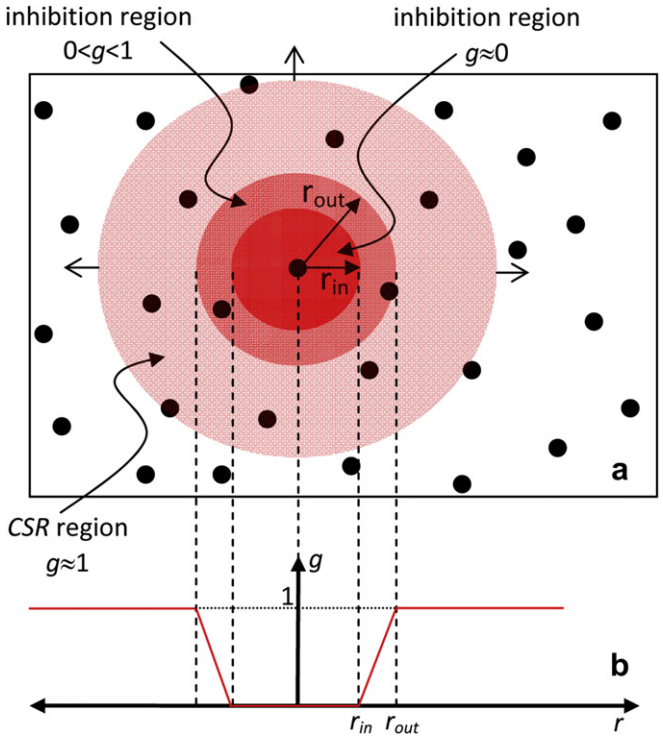

Fig. 9. a) Schematic diagram of the electroperforation process (top view) and distances involved. g is the pair correlation function and r_{in} and r_{out} the inner and outer radius of the soft inhibition potential. b) Pair correlation function g as a function of the generic distance r. The value g 1 corresponds to a CSR process.

2.2. Conclusion

The spatial distribution of holes in paper sheets generated by means of electrical discharges was investigated. It was shown that for the given experimental conditions there is a maximum number of holes that can be generated in a certain area because of the lower impedance paths offered by the already made holes. This originates a deviation from complete spatial randomness at short length scales, which is characterized using an spatial inhibition potential. For another experimental conditions (distance between electrodes, paper type, etc.) the size of the inhibition region may change. The issue was investigated using direct distance methods and summary function statistics, but mainly using the pair correlation function. Thanks to this statistical tool, it has been possible to establish for the given experimental conditions the range of distances in which complete and partial inhibition of the hole generation process occurs.

Acknowledgment

This work was supported by the Ministerio de Ciencia e Inno vación of the Spanish Government under the project TRACE TRA2009 0119.

References

[1] C.J.M. van Rijin, Nano and Micro Engineered Membrane Technology, Elsevier, 2004.
[2] J. García-García, E. Miranda, C. Martínez-Cisneros, J. Alonso, J. Elec 68 (2010) 196 199.
[3] J. Illian, A. Penttinen, H. Stoyan, D. Stoyanet, Statistical Analysis and Modelling of Spatial Point Patterns, Wiley, 2008.
[4] N. Cressie, Statistics for Spatial Data, Wiley Series in Probability and Statistics, Wiley, 1993.
[5] E. Miranda, C. Garzón, C. Martínez-Cisneros, J. Alonso, J. García-García, J. Phys. Conf. Ser. 301 (2011) 012049.
[6] J. García-García, E. Miranda, C. Garzón, C. Martínez-Cisneros, J. Alonso, IEEE-Industry Applications Society Annual Meeting (IAS) (2010) 1 4.
[7] A. Baddeley, R. Turner, Journal of Statistical Software 12 (2005) 1 42.
[8] A. Mathai, P. Moschopoulos, G. Pederzoli, Rendiconti del Circolo Matematica di Palermo, Serie II, Tomo XLVIII (1999) 163 190.